Pergamon

*Journal of Structural Geology*, Vol. 16, No. 4, pp. 519 to 530, 1994

0191-8141/94 $6.00+0.00

# Assessing brittle volume-gain and pressure solution volume-loss processes in quartz arenite

CHARLES M. ONASCH

Department of Geology, Bowling Green State University, Bowling Green, OH 43403, U.S.A.

(*Received* 15 *January* 1993; *accepted in revised form* 15 *September* 1993)

**Abstract**—Quartz arenite of the Tuscarora Sandstone has been deformed by dislocation flow, pressure solution and microfracturing of which the last two are most important. Pressure solution involved shortening with no extension. Most samples have approximately 20% shortening normal to bedding interpreted to be compaction, and a few have up to 20% layer-parallel shortening of tectonic origin. Because there is no extension, these shortenings resulted in an equivalent amount of bulk volume loss. Multiple sets of microfractures in the form of fluid inclusion planes and microveins account for up to 10% extension and bulk volume increases up to 17%. When both microfracture volume gains and pressure solution volume losses are considered together, all samples show a net bulk volume loss ranging from 14 to 35%. Changes in material volume are different than bulk volume because of the presence of porosity at the time of pressure solution. Whereas all samples show bulk volume losses, most samples show net material volume gains of up to 16% with only those having experienced both compactional and tectonic pressure solution showing material volume losses.

Pressure solution during compaction can account for most but not all cement. Compactional pressure solution surfaces do not extend into pore-filling cement suggesting that much of the cement was externally derived after compaction. Therefore, the flux of material may have been considerably greater than the material volume changes would indicate.

## INTRODUCTION

DESPITE a rapid growth of methods for determining finite and incremental strains, the measurement of volume changes remains elusive. This difficulty arises because, unlike many finite strain methods which measure ratios of the principal extensions, volume strains require measurement of the extensions themselves. The paucity of volume change data is unfortunate because there is a growing controversy over whether deformation can be accompanied by significant volume changes (e.g. Ague 1991, Wintsch *et al.* 1991, Wright & Henderson 1992).

To date, most studies of volume changes have dealt with the effects of pressure solution which is a major deformation mechanism in sedimentary and low-grade metamorphic rocks (Kerrich 1977). In argillaceous rocks, up to 50% of the volume may have been removed by pressure solution (Wright & Platt 1982, Beutner & Charles 1985, Henderson *et al.* 1986, Wright & Henderson 1992). In graywacke sandstones (Brandon *et al.* 1991), conglomerates (Mosher 1987) and limestones (Alvarez *et al.* 1978), proposed volume losses are nearly as large.

Considerably less attention has been focused on volume-gain deformation even though it is generally acknowledged that many brittle processes will produce a volume increase (e.g. Sibson 1987). Any type of fracture that has a component of opening will result in a volume increase. Although brittle strains have been quantified (Wojtal 1986, 1989, Jamison 1989, Marrett & Allmendinger 1990), only recently have associated volume increases been considered (Onasch 1990).

When considering volume changes, a distinction must be made between bulk volume changes and material volume changes. The former describes geometric changes in the rock mass whereas the latter deals with changes in the volume of material. The two will be different if porosity exists at the time of deformation. For example, the destruction of porosity by pressure solution during compaction can result in a significant bulk volume loss. Material volume changes will be smaller and can vary depending on whether the material released by pressure solution remains as cement (Houseknecht 1988) or is removed from the rock (Sibley & Blatt 1976, Wilson & Sibley 1978).

The purpose of this paper is to assess the magnitude and timing of volume changes experienced by a quartz arenite with a relatively simple deformational history. The strains associated with the dominant deformation mechanisms, pressure solution and microfracturing, have been quantified and volume changes determined along with their timing. Quartz arenite is ideal for this type of study because its simple mineralogy eliminates grain-scale variations in strain and deformation mechanisms caused by compositional differences.

### *Geologic setting*

Samples for this study are from the Lower Silurian Tuscarora Sandstone and its correlative the Massanutten Sandstone exposed in the Appalachian foreland fold and thrust belt. The thrust belt is divided into central and southern segments by a reentrant in Virginia (Fig. 1).

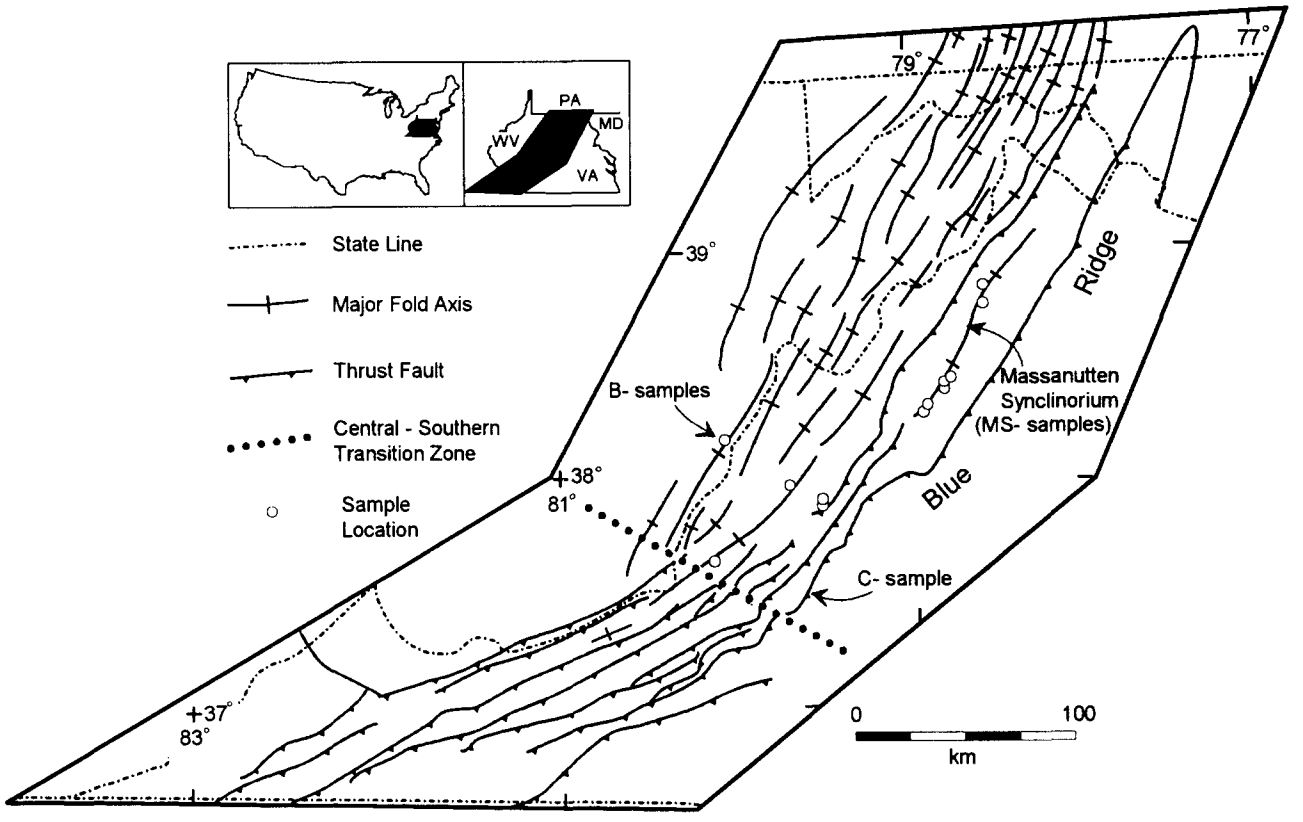


Fig. 1. Generalized tectonic map of portion of the Appalachian fold and thrust belt showing major structural elements and location of samples used in study. Transition zone between central and southern Appalachians centered about bold dotted line. Map modified from Hatcher *et al.* (1989).

The sandstone occurs in the macrofolded roof sequence of the central Appalachians and in the thrust system of the southern Appalachians. Separating the two regions is a transition zone where it occurs in both roof and thrust system. Deformation occurred in a diachronous fashion during the Alleghanian orogeny with thrusting in the southern Appalachians having initiated prior to that in the central Appalachians (Geiser & Engelder 1983, Dean *et al.* 1988, Hatcher *et al.* 1989).

The Tuscarora Sandstone is a medium-grained, framework-supported quartz arenite 30–150 m thick. Quartz comprises over 95% of the framework components with overgrowth quartz cement and a trace of clay completely filling the intergranular volume leaving virtually no porosity. Temperatures during deformation were everywhere less than 200°C with a general east to west decrease (Epstein *et al.* 1977, Harris 1979, Epstein 1988). Finite strains are low with $X/Z$ ratios ranging from 1.10 to 2.00 (Onasch 1991, Couzens *et al.* 1993).

Samples of Massanutten Sandstone (MS sample numbers) are from vertical to overturned limbs of the Massanutten synclinorium, a tight macrofold in the roof sequence of the central Appalachians (Fig. 1). The Tuscarora samples (B sample numbers) are from moderate to gently-dipping limbs of macrofolds in the central Appalachians along a cross-strike traverse approximately halfway between the southern end of the Massanutten synclinorium and the central-southern Appalachian transition zone (Fig. 1). Sample C-3 is from a moderately-dipping fold limb in the transition zone (Fig. 1).

*Deformation mechanisms*

Microstructures indicate that grain-scale deformation in the Tuscarora Sandstone occurred by three mechanisms: dislocation flow, pressure solution and microfracturing (Onasch & Dunne 1993). Dislocation flow microstructures include undulatory extinction, deformation lamellae and deformation bands. In the Massanutten synclinorium, grain boundary recrystallization is present locally in high strain zones (Onasch 1991). Pressure solution is manifested primarily by sutured and interpenetrated detrital grains (Figs. 2a & b), and less commonly, by transgranular stylolites. Microfractures include fluid inclusion planes (FIPs), microveins and cataclastic bands. FIPs are healed Mode I fractures (Lawn & Wilshaw 1975) decorated with fluid-filled inclusions 0.4–5.0 $\mu$m in diameter (Fig. 2c). Microveins, which occur in sets parallel to the FIPs, are also Mode I fractures, but have widths between 10 and 200 $\mu$m (Figs. 2d & e). The quartz filling microveins is in optical continuity with wallrock grains making it difficult or impossible to see in transmitted light, but it is clearly visible in cathodoluminescence (compare Figs. 2d & e). Microveins cross both detrital grains and overgrowth cement indicating that they post-date cementation. In some samples, microveins are slightly offset along sutured grain boundaries which extend through the microvein indicating that pressure solution was coeval with or younger than microfracturing (Fig. 2d). Of the three deformation mechanisms, pressure solution and microfracturing are believed to be the most important in

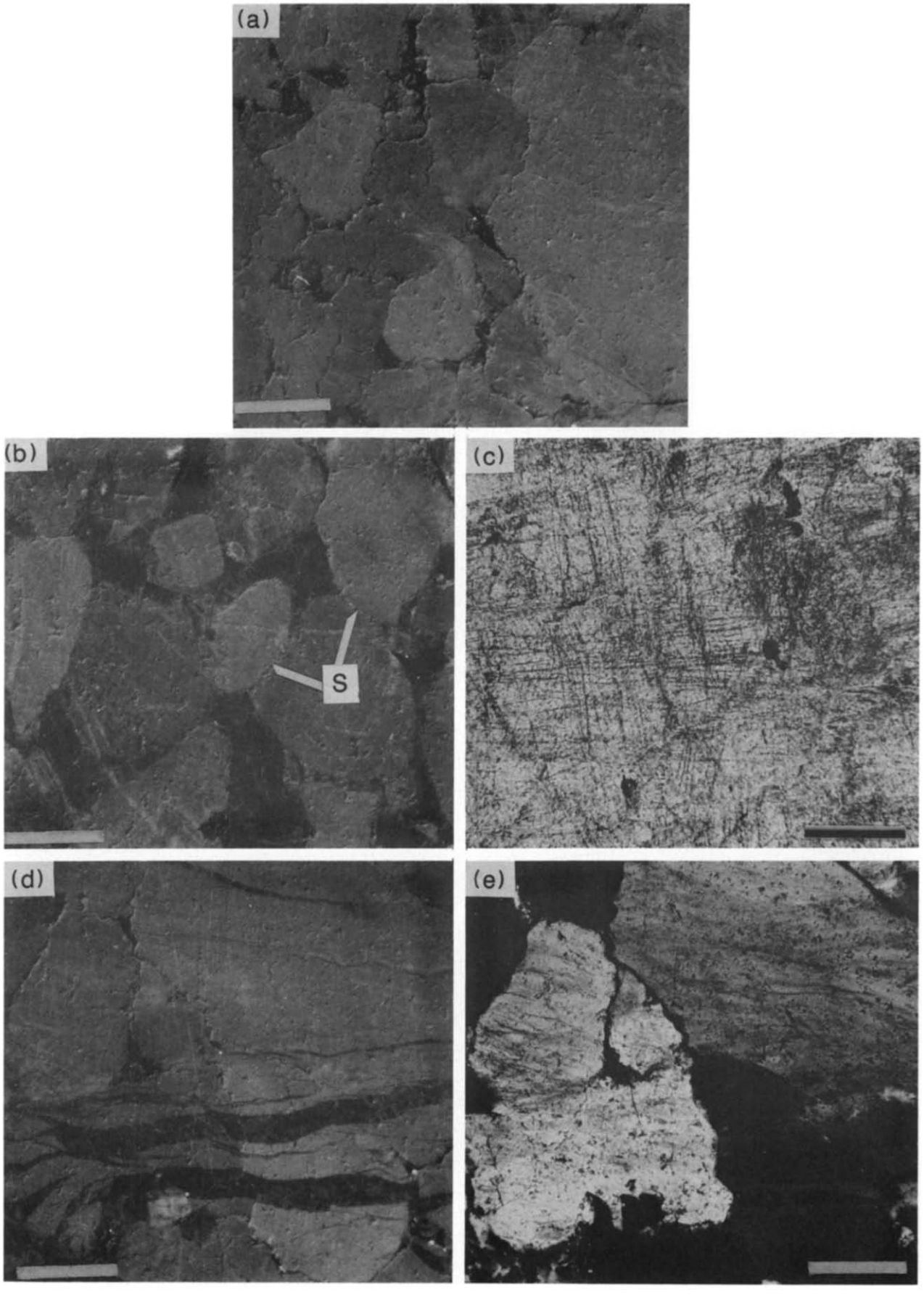


Fig. 2. Photomicrographs of pressure solution and brittle microstructures in the Tuscarora Sandstone. (a) Interpenetrated detrital grains in cathodoluminescence. (b) Detrital grains with dark luminescing quartz cement filling intergranular volume. Note that sutured pressure solution surfaces (s) between detrital grains do not extend into cement or along cement–detrital grain boundary. (c) Orthogonal fluid inclusion planes (FIPs) in plane light. (d) Microveins in cathodoluminescence. Sutured grain boundaries indicate horizontal shortening which is consistent with vertical opening direction of microveins suggesting that pressure solution and microfracturing are coeval. (e) Same view as (d), but in polarized light. Note difficulty in recognizing microveins in polarized light. Cathodoluminescence photomicrographs taken on Technosyn cathodoluminescence microscope operating at 20 kV and 500 mA. Scale bar in each photomicrograph is 0.2 mm.

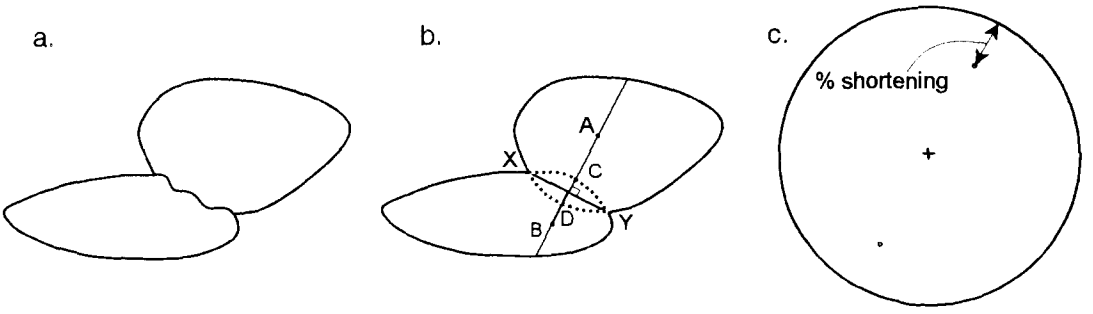


Fig. 3. Determination of pressure solution strain (PSS) from geometry of interpenetrated grains. (a) Two grains showing effects of pressure solution shortening. (b) Quantities used in constructing PSS plot. Dotted lines are reconstructed grain boundaries. XY is compromise boundary; AB is normal to XY at its midpoint; A and B are midpoints of each grain along line AB; and C and D are intersections of AB with reconstructed grain boundaries. (c) PSS plot for two grains in (a). Distance between points and perimeter of circle is proportional to percent shortening along line AB. Radius of circle corresponds to state of no strain.

their contribution to the finite strain (Onasch 1990, Onasch & Dunne 1993).

## METHODS

### *Pressure solution*

Pressure solution strains (PSS) were determined from the geometry of interpenetrated and truncated grains. During pressure solution, grains are displaced as rigid bodies parallel to the shortening direction (Durney 1976). As a grain comes in contact with its neighbor, material is removed from one or both grains. The geometry of the contact is a function of the original position of the grains relative to the shortening direction and the amount of shortening. Using these relations, the magnitude and direction of pressure solution shortening can be determined as follows. Where two grains have interpenetrated (Fig. 3a), a compromise boundary is drawn (XY in Fig. 3b) by reconstructing the original grain boundaries (dotted lines). A line (AB) is drawn normal to this boundary at its midpoint and a point halfway across the original width of each grain is located on this line (A and B), along with the intersections of the overlap segments and the line (C and D). From the original distance between grains (AB + CD) and the present distance (AB), the shortening along line AB can be calculated. For grains truncated against a dissolution surface (e.g. cleavage selvage), the shortening can be calculated by reconstructing the original grain shape and measuring the original grain dimension and the present dimension along a line normal to the surface.

The shortening is shown graphically on a circle whose radius corresponds to a state of no strain by plotting a point a distance in from the perimeter of a circle proportional to the shortening along a line parallel to AB (Fig. 3b). A second point can be plotted 180° away because the shortening does not have a unique direction. By making these measurements on a number of grains, a PSS plot can be constructed from which the magnitude and direction of the bulk pressure solution shortening can be determined by fitting an ellipse to the central vacancy in the same manner as a Fry diagram. The PSS method can also be used where pressure solution-related extension in the form of beards or overgrowths has occurred in which case points would plot outside the circle in the PSS plot.

The ability of the PSS method to accurately determine the pressure solution strain depends on: (1) reconstructing the original grain shapes; (2) fitting an ellipse to the central vacancy; (3) the packing of the grains; and (4) knowing that grain interpenetrations are due to pressure solution, not plastic deformation. Original grain shapes were reconstructed so that the shapes are consistent with other grains in the population. With the well-rounded grains in the Tuscarora Sandstone this is generally not a problem. Visually fitting an ellipse to the central vacancy is subjective, but can be made more reproducible by using at least 50–75 grain pairs. Packing determines whether the actual shortening or minimum shortening is determined. For framework supported rocks, such as the Tuscarora Sandstone, the PSS method yields the true shortening, whereas for matrix-supported rocks, like graywackes, it would be a minimum shortening. The PSS method will yield only the pressure solution strains, even where other mechanisms such as grain-boundary sliding, microfracturing or plastic deformation are operating coevally. The exception to this is where plastic deformation results in grain interpenetrations similar to those produced by pressure solution (Atkinson & Rutter 1975, Deelman 1975) in which case some of the strain recorded by the method will be plastic deformation. However, plastic grain interpenetrations would form in ductile grains and not the quartz grains of the Tuscarora Sandstone. Using simulated coaxial and non-coaxial pressure solution deformation of a variety of marker shapes and packing arrangements, the PSS method has proven reliable for between 5 and 50% (Onasch in press). Accuracy was generally within ±5% for coaxial shortenings up to 30% and ±10% for non-coaxial shortenings.

Complete interpretation of pressure solution strains requires the use of non-parallel sections due to the effects of shortening on three-dimensional objects. For example, vertical shortening of a grain aggregate with no horizontal extension produces interpenetrations in a vertical plane, but in a horizontal plane as well (Fig. 4).

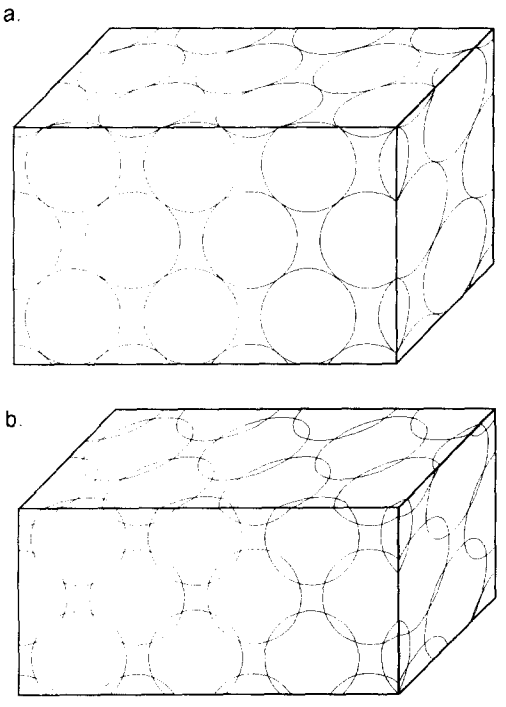


Fig. 4. Block diagrams illustrating true and apparent shortening on rhombohedrally-packed spheres. (a) Block diagram of rhombohedrally-packed spheres. (b) Same block after 20% vertical shortening with no horizontal extension. Overlaps on horizontal plane are apparent shortening whereas overlaps on vertical sides are due to true shortening.

In planes parallel to the shortening direction, the shortening is the true shortening. The shortening in any other plane is an apparent shortening because there has been no bulk shortening in that direction, only crowding of the grains caused by the displacements parallel to the shortening direction. The magnitude of apparent shortening relative to true shortening depends on the packing arrangement, sorting, and amount of true shortening (Onasch in press). For the Tuscarora Sandstone, the apparent shortening will be equal to or less than the true shortening. Apparent shortening can be differentiated from true shortening on a PSS plot because the former shows equal shortening in all directions whereas the latter has indicates only one shortening direction. If pressure solution included a component of extension, apparent shortening would be asymmetrical, but would still show some shortening in all directions compared to a single direction for true shortening.

For the Tuscarora Sandstone samples, PSS plots were constructed from grain interpenetration geometries measured on three mutually-perpendicular thin sections. At least 75 grains were measured in each section. Cathodoluminescence was used to identify detrital grain outlines and grain interpenetrations because the grains cannot be differentiated from their optically continuous cement in plane or polarized light. Interpretation of the PSS plots required distinguishing true vs apparent shortening using the criteria above and constructing a strain geometry that was consistent for each of the three perpendicular sections. In the samples used in this study, interpretation was simplified by the fact that the shortening directions coincided with the three perpendicular sections.

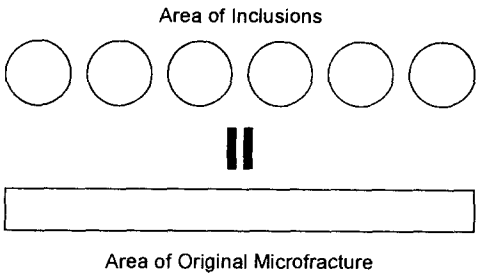


Fig. 5. Assumption used in calculating extensional strains for FIPs. Area of inclusions is same as area of original microfracture.

*Microfracturing*

Extensional strains were determined from the geometry of FIPs and microveins using the method described by Onasch (1990). For FIPs, the inclusion diameter and inclusion spacing along an inclusion plane was used to calculate the total area of inclusions for that plane. Assuming that the area of inclusions in the plane is equal to the area of the original microfracture (Fig. 5), the width of the original microfracture can be determined. From the width of the microfracture, along with the microfracture spacing, the extensional strain normal to a number of microfractures can be calculated. The method is a conservative estimate of the strain because the area of inclusions (trapped fluid) may be less than the original microfracture (e.g. Lloyd & Knipe 1992, fig. 2e). Also, underestimation of the strain will result if microfractures heal without trapping any inclusions.

For microveins, extensional strains were measured along thin section traverses normal to the microveins. The total width of microveins and the length of the traverse were used to calculate the extensional strain. For samples with multiple sets of microveins, this procedure was repeated for each set. All measurements of microveins must be done in cathodoluminescence, because quartz in the microveins is in optical continuity with the wallrock grains (compare Figs. 2d & e).

## RESULTS

*Pressure solution*

Pressure solution shortening measured in seven samples of the Tuscarora Sandstone is shown in Table 1 and as block diagrams and PSS plots for three representative samples in Figs. 6–8. Pressure solution did not involve any extension as no beards or tectonic overgrowths are present. With one exception, the samples show shortening normal to bedding of approximately 20% (Table 1) as illustrated in Fig. 6(a). PSS plots for bedding-normal sections show a single shortening direction (Figs. 6c & d). In the bedding plane, equal shortening in all directions is indicated by the PSS plot (Fig. 6b); however, this is interpreted to be apparent shortening

Table 1. Pressure solution shortening and volume changes

| Sample | Shortening direction | % shortening | % volume change for sample |
|---|---|---|---|
| B-1 | Bedding-normal | 22.0 | |
| | LPS, strike-parallel | 19.0 | −36.8 |
| B-3 | Bedding-normal | 18.5 | −18.5 |
| B-6 | Bedding-normal | 18.0 | −18.0 |
| B-10 | Bedding-normal | 19.0 | −19.0 |
| C-3 | Bedding-normal | 19.0 | −19.0 |
| MS-28 | LPS, strike-normal | 18.5 | |
| | LPS, strike-parallel | 14.0 | −38.0 |
| MS-188 | Bedding-normal | 26.0 | |
| | LPS, strike-normal | 20.0 | −40.8 |

resulting from the true shortening normal to bedding. Shortening normal to bedding is believed to be a result of sedimentary compaction that dominates the finite strain in the Tuscarora of the central Appalachians (Couzens *et al.* 1993).

In addition to compaction, three samples show layer-parallel shortening (LPS) by pressure solution (Table 1); one normal to strike (MS-188, Fig. 7), one parallel to strike, and one with both directions (MS-28, Fig. 8). In MS-188, PSS plots from both bedding-normal sections show 26% shortening normal to bedding interpreted to be compaction (Figs. 7b & c). In the bedding-parallel section, 20% LPS normal to strike is indicated (Fig. 7d). The small shortening parallel to strike shown on the PSS plots is interpreted to be apparent shortening resulting from the two true shortening directions. MS-28 is unusual in that it shows two directions of LPS and no compaction (Fig. 8a). Strike-normal LPS and a lack of compaction are evident on the PSS plot for the vertical, strike-normal section (Fig. 8c). PSS plots from the other sections show the effects of LPS parallel to strike as well as apparent shortening (Figs. 8b & d). Strike-normal LPS is common in the central Appalachians (Geiser & Engelder 1983), but strike-parallel LPS is not. The location of MS-28 in an area of rapid plunge change may explain the shortening parallel to strike.

Volume changes due to pressure solution were calculated from the shortening values (Table 1). Because there is no evidence for pressure solution-related extension, the shortening resulted in a bulk volume loss. Where only compaction occurred, the volume loss is equal to the shortening. Where two orthogonal shortening directions were found (e.g. Figs. 7 and 8), they were treated as principal extensions and used to calculate the volume loss according to:

$$(1 + \Delta) = (1 + e_x)(1 + e_y)(1 + e_z) \qquad (1)$$

(modified from Ramsay & Wood 1976, equation 2).

Volume losses range from 18% in samples with only compactional pressure solution to 40.8% in samples with both compactional and tectonic pressure solution (Table 1).

*Microfracturing*

Extensional strains determined from FIPs and microveins in 11 samples of the Tuscarora Sandstone are shown in Table 2. In most samples, at least two orthogonal sets of FIPs (Fig. 8) and microveins are present. The orientation of microfracture sets is remarkably uniform over a wide area in the central and southern Appalachians with three sets being present: horizontal (Set I); vertical, strike-normal (Set II); and vertical, strike-parallel (Set III).

In most samples, extension due to FIPs is greater than that due to microveins with FIP strains ranging from 0 to 6.1% compared to those for microveins which range from 0 to 5.2% (Table 2). Total microfracture extensions reach almost 10% for individual sets. No microfracture set had consistently higher or lower strains than the others.

Volume gains for each sample were calculated from the total extensions for each microfracture set. Because the multiple sets are orthogonal (e.g. Fig. 8), the extensions were treated as principal extensions from which dilation can be calculated by equation (1). Volume gains range from 0% in samples with no microfractures to 17.1% in samples with intense microfracturing (Table 2).

## NET VOLUME CHANGES

The Tuscarora Sandstone has been deformed by both volume-gain and volume-loss processes. Determination of the net bulk volume change requires integration of the microfracture strains with the pressure solution strains. Dislocation flow, which is relatively unimportant as a deformation mechanism (Onasch & Dunne 1993), is a constant-volume process and therefore need not be considered in assessing the net volume change. The net bulk volume change was calculated by first finding the extensions in the three principal directions. Once the principal extensions were determined, the bulk volume change can be calculated according to equation (1).

Each of the six samples where both microfracture and pressure solution strains were measured shows a net bulk volume loss of between 14.1 and 35.2% (Table 3). The largest losses are in samples MS-188 and B-1 which underwent both compactional and tectonic pressure solution. Even the sample with the highest microfracture volume gains (MS-28) shows significant net bulk volume loss because it also has a large pressure solution volume loss.

*Bulk volume change vs material volume change*

All of the samples in which pressure solution and microfracture strains were measured show significant net bulk volume losses. However, in porous rocks such as sandstones, a net loss in bulk volume may not lead to a net loss of material volume. Differences arise because material dissolved by pressure solution can fill pores and remain in the system. The controlling factors are the amount of porosity present at each stage in the deformation and whether material dissolved by pressure solution remains in the rock as pore or vein fillings (closed

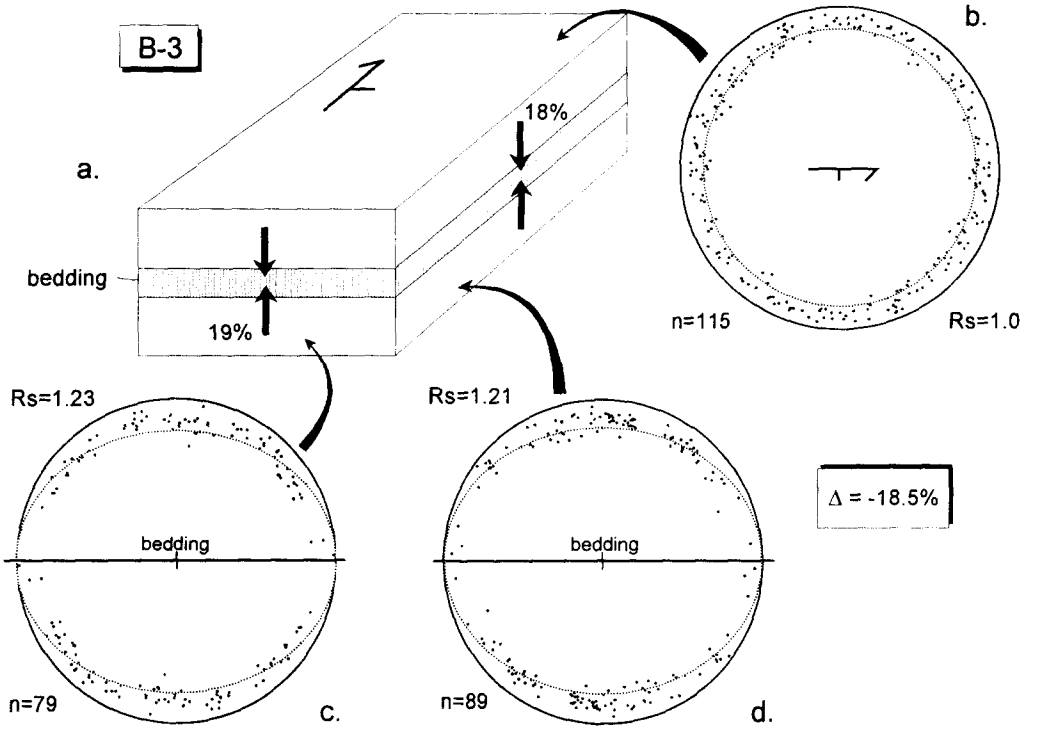


Fig. 6. Block diagram and PSS plots summarizing pressure solution and microfracture strains in sample B-3. (a) Block diagram showing relations between bedding (stippled layer), microfractures (black bands), and shortening and extension directions (arrows). (b) PSS plot for horizontal plane. (c) PSS plot for vertical, strike-normal section. (d) PSS plot for vertical, strike-parallel section. Dotted ellipse in each PSS plot describes pressure solution shortening. Only true shortening shown on block diagram.

system) or leaves the system (open system). Where porosity is present at the time of pressure solution, the material volume loss will be less than the bulk volume loss. Where there is no porosity, the material volume loss will be equal to the bulk volume loss.

When discussing sandstones, it is important to distinguish between intergranular volume, which is the space between the framework grains, and porosity, which is open intergranular volume. The former is a geometric descriptor whereas the latter is a function of

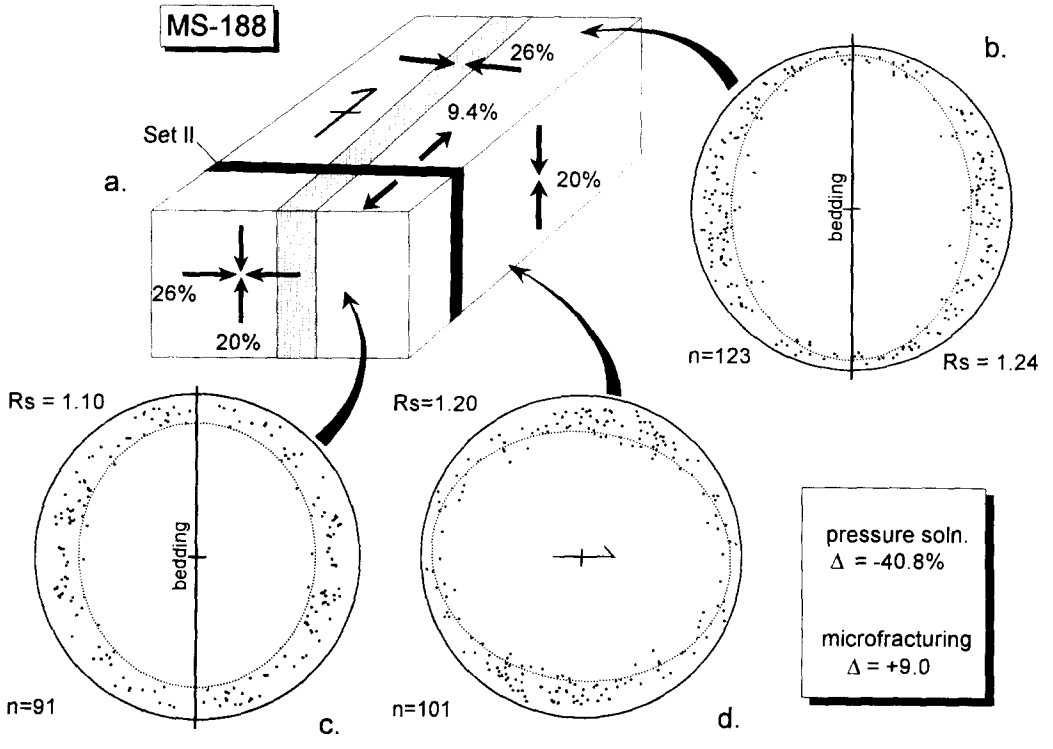


Fig. 7. Block diagram and PSS plots summarizing pressure solution and microfracture strains in sample MS-188. Description same as for Fig. 6.

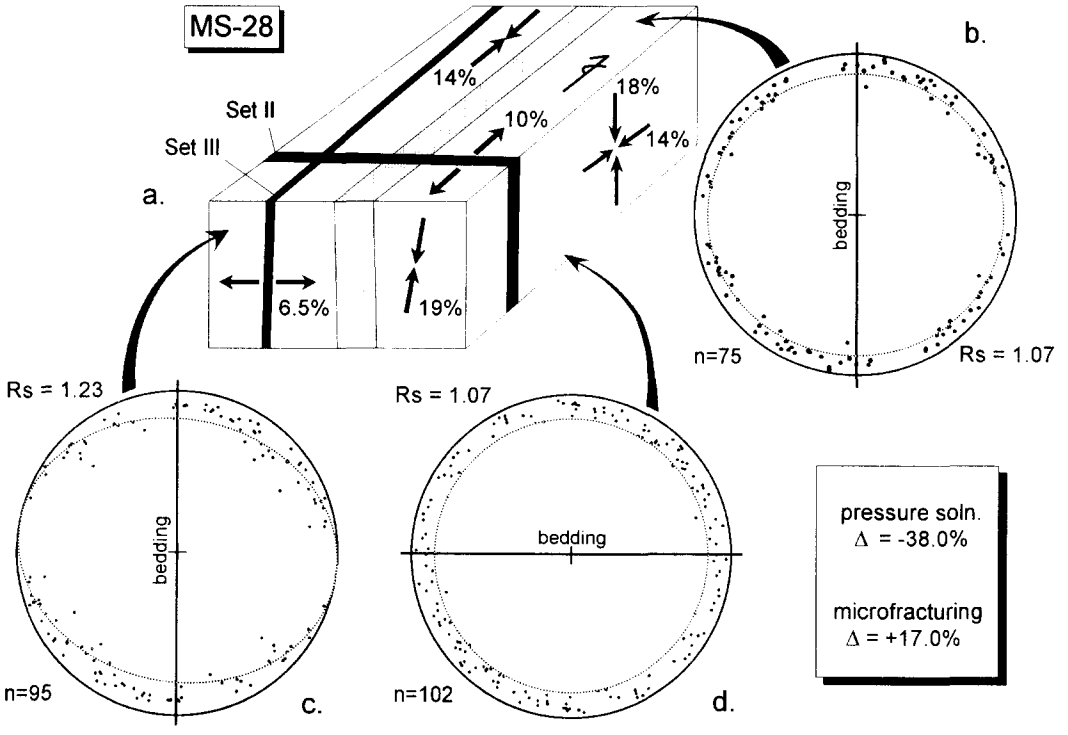


Fig. 8. Block diagram and PSS plots summarizing pressure solution and microfracture strains in sample MS-28. Description same as for Fig. 6.

whether cement is present or absent in the intergranular volume. Well sorted sands at the sediment–water interface have an average porosity of 40% (Graton & Frasier 1935, Gaither 1953, Beard & Weyl 1973). With burial, they are mechanically compacted to about 30% porosity (Heald 1956, Manus & Coogan 1974). Any additional compaction must occur by pressure solution or plastic deformation of framework grains with the latter being unimportant in a quartz arenite (Houseknecht 1988).

The amount of material released by pressure solution and change in intergranular volume are controlled by the shortening and initial intergranular volume. To investigate the relationship, computer simulations of pressure solution deformation were done on grain outlines traced from a photomicrograph of well-sorted, medium-grained sand mechanically compacted to 30% porosity. This aggregate was subjected to increasing amounts of pressure solution deformation simulated by

Table 2. Microfracture extensional strains and volume changes

| Sample | Microfracture set* | % extension | | | % volume change for sample |
|---|---|---|---|---|---|
| | | FIP | Microvein | Total | |
| B-1 | I | 0.6 | 0 | 0.0 | |
| | II | 0.8 | 0.1 | 0.9 | |
| | III | 1.8 | 0.7 | 2.5 | 4.0 |
| B-3 | none | — | less than 0.5 | — | 0 |
| B-6 | I | 1.4 | 0 | 1.4 | |
| | III | 1.1 | 1.3 | 2.4 | 3.8 |
| C-3 | I | 0.5 | 1.2 | 1.7 | |
| | II | 1.4 | 1.4 | 2.8 | |
| | III | 0.9 | 0.6 | 1.5 | 6.1 |
| MS-28 | II | 4.7 | 5.2 | 9.9 | |
| | III | 4.7 | 1.8 | 6.5 | 17.1 |
| MS-68 | II | 3.8 | 1.4 | 5.2 | |
| | III | 5.5 | 0.7 | 6.2 | 11.7 |
| MS-78 | II | 2.9 | 2.6 | 5.5 | |
| | III | 3.9 | 3.1 | 7.0 | 12.8 |
| MS-79 | I | 4.3 | 0.3 | 4.6 | |
| | II | 0.4 | 0.2 | 0.6 | 5.2 |
| MS-165 | II | 5.5 | 0.4 | 5.9 | |
| | III | 4.2 | 0.9 | 5.1 | 11.2 |
| MS-188 | II | 5.9 | 3.5 | 9.4 | 9.4 |
| MS-196 | I | 6.1 | 2.9 | 9 | |
| | II | 2.6 | 1.1 | 3.7 | 13.0 |

*Set I—horizontal; Set II—vertical, strike-normal; Set III—vertical, strike-parallel.

Table 3. Percent net volume changes for samples where both pressure solution and microfracture strains were measured. Conditions for material volume cases A and B described in text

| | | Material volume | |
|---|---|---|---|
| Sample | Bulk volume | Case A | Case B |
| MS-28 | −17.9 | 15.1 | −17.9 |
| MS-188 | −35.2 | −7.1 | −12.5 |
| B-1 | −34.7 | −5.5 | −16.2 |
| B-3 | −18.5 | 10.5 | n/a |
| B-6 | −14.9 | 14.3 | n/a |
| C-3 | −14.1 | 16.1 | n/a |

n/a—not applicable.

displacing the grains as rigid bodies parallel to the shortening direction. After each shortening increment, the overlap and intergranular volumes were determined from 1000 point-counts of grain overlaps and intergranular areas, respectively, and plotted against the shortening (Fig. 9).

The curves show that the amount of grain overlap and intergranular volumes vary non-linearly with shortening. A similar relationship was found in a theoretical study of the effects of pressure solution on porosity in three-dimensional aggregates of packed spheres (Mitra & Beard 1980). For shortening values of less than approximately 28%, the intergranular volume can accommodate all material released by pressure solution (overlap volume). Above 28% shortening, there is not enough intergranular volume and material must be removed from the system. Assuming that all the intergranular volume was open at the time of pressure solution, the 20% compaction experienced by the Tuscarora Sandstone would result in a 10% overlap volume (Fig. 9). Because all of this material could be accommodated in the intergranular volume, the amount of material volume loss may be significantly less than the bulk volume losses in Table 3.

The curves in Fig. 9 also provide an independent check on the shortening values determined by the PSS method. From point-counting, the average intergranular volume for the Tuscarora samples which have experienced only compactional pressure solution is 16%. According to Fig. 9, this corresponds to a shortening of approximately 23% compared to the 20% determined from the PSS method. This small difference may be due to initial intergranular volumes of the model being different from that of the Tuscarora.

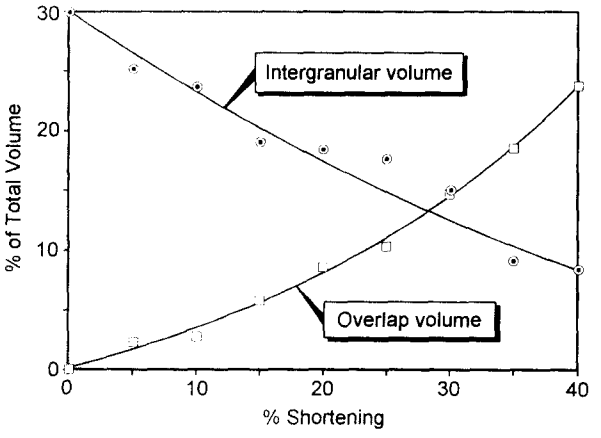


Fig. 9. Variation in overlap and intergranular volumes with shortening for simulated pressure solution deformation of sand grains with 30% initial porosity.

Material volume changes were calculated for two cases using the curves in Fig. 9 to determine the amount of material released by pressure solution and intergranular volume remaining after shortening. These, along with the volume of material filling microfractures, give the net material volume change. For the calculations, it was assumed that the maximum open intergranular volume at the time of compaction was 30% and was completely filled prior to tectonic deformation.

The first case (A in Table 3) assumes that all material released by compactional and tectonic pressure solution remains in the system to fill porosity and/or microfractures. Whereas all samples showed large bulk volume losses, only two show a net material volume loss and four show net gains (Table 3). Samples with high microfracture density (MS-28) and/or small amounts of pressure solution (B-6) require material to be imported to fill the porosity and microfractures. Samples with both compactional and tectonic pressure solution (MS-188 and B-1), have an excess of material even after filling all porosity and microfractures.

The second case (B in Table 3) considers whether tectonic pressure solution alone is sufficient to fill the microfractures. It assumes that all intergranular volume is cemented prior to tectonic deformation and that there is coupling between tectonic pressure solution and microfracture filling (Cox & Ethridge 1989). Microveins propagate across both framework grains and cement (Fig. 2d); therefore, the intergranular volume must have been completely cemented prior to microfracturing. The orthogonal relationship between microfracture sets and pressure solution shortening directions (Figs. 6b & c) is suggestive of coupling. Because there is no porosity at the time of deformation, the material volume change will be the same as the bulk volume change. The three samples with both tectonic pressure solution and microfractures show a net material volume loss (Table 3). Tectonic pressure solution is more than sufficient to fill the microfractures.

## DISCUSSION

Compaction is not always included when investigating the deformational history of a rock because it is not considered tectonic in origin; yet, it has several important consequences. In low strain rocks like the Tuscarora Sandstone, it can be the dominant process in determining the finite strain (Couzens *et al.* 1993). Even in rocks with strong tectonic fabrics, it must be considered to completely understand the finite strain (Oertel 1970, Sanderson 1976, Chandra *et al.* 1977, Boulter 1983,

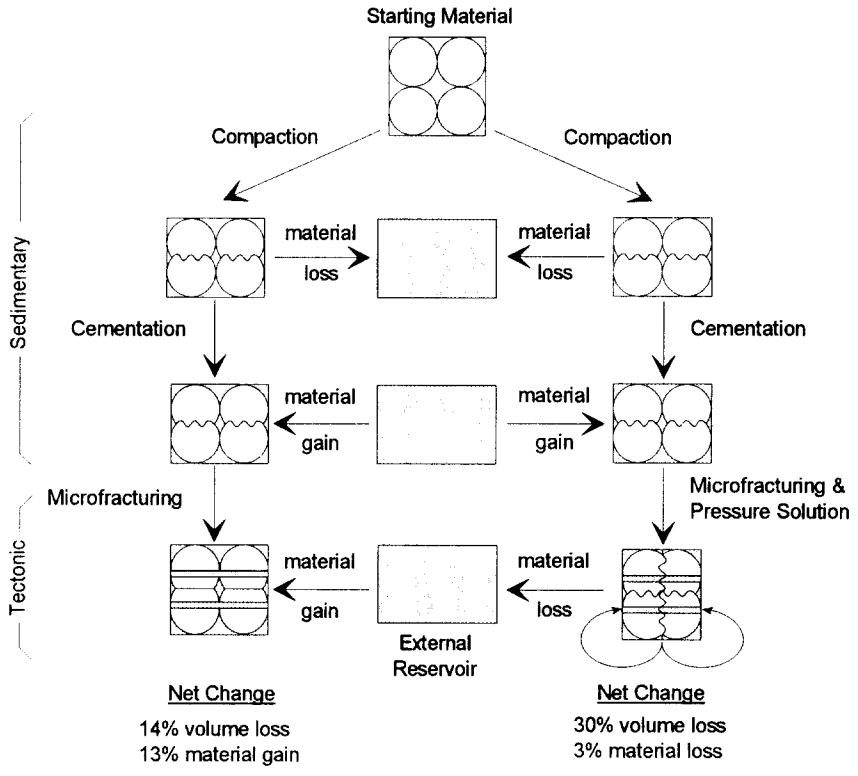


Fig. 10. Volume change histories for Tuscarora Sandstone. Starting material is sand mechanically compacted to 30% porosity. Left column of diagram is for samples with no tectonic pressure solution. Right column is for samples with tectonic pressure solution. Net changes at bottom are averages. Wavy lines are pressure solution surfaces and stippled bands are filled extensional microfractures.

1986). Compaction and associated porosity reduction are also responsible for the differences between bulk volume and material volume losses.

Like many sandstones, cement in the Tuscarora Sandstone is believed to have been derived by pressure solution, either *in situ* or in adjacent units (Sibley & Blatt 1976, Houseknecht 1988). While Houseknecht (1988) found a general balance between the cement and grain overlap volumes, Sibley & Blatt (1976) found that there was not enough overlap volume and hence, a need for an external source for part of the cement. Using the PSS shortening values and the curves in Fig. 9, the amount of cement produced by compactional pressure solution falls short by 10–20% in filling the present intergranular volume. Therefore, this study also indicates a need for an external source of cement. Only in the two samples with large amounts of tectonic pressure solution (MS-188 and B-1) is there an adequate amount of pressure solution to fill the intergranular volume.

The material volume changes determined from geometric arguments done in this study are minimum estimates of the flux of material through the system. A sample with a small change in material volume could have experienced a large material flux if internally-derived material was replaced by an equivalent amount from an external source. This may be the case in the Tuscarora Sandstone. Textural evidence in samples which have undergone only compactional pressure solution argues that the silica released during compaction did not remain locally in the pores. In these samples, pressure solution surfaces between detrital grains generally do not propagate into the pore-filling cement or along the cement–grain contact (Fig. 2b) as would be expected if cement was being precipitated coevally with pressure solution. Sibley & Blatt (1976) and Wilson & Sibley (1978) also argue that much of the pressure solution that occurs during compaction predates any cementation because if cement were present, it would inhibit pressure solution by lowering the grain-to-grain stress concentrations. Therefore, it seems likely that material dissolved during compaction in the Tuscarora Sandstone was removed from the system and that the pores were filled from an external source subsequent to compaction. Although this would have no effect on the net change in material volume, it greatly increases the flux of material.

## SUMMARY

This study supports the idea that deformation can result in a significant change in volume. All samples show a net bulk volume loss; however, when initial porosity is taken into account, all except those with tectonic pressure solution show a net material volume gain. Figure 10 summarizes the volume change history of the Tuscarora Sandstone for samples with and without tectonic pressure solution. Starting as sand mechanically compacted to 30% porosity, all samples underwent compactional pressure solution with material loss followed by cementation with the cement derived from an external reservoir (left and right columns, Fig. 10). For

samples with no tectonic pressure solution, any microfractures that formed were filled from an external source (left column fig. 10). The net effect of these processes is an average of 14% bulk volume loss and 13% material volume gain. Following compaction and cementation, samples with tectonic pressure solution underwent coupled microfracturing and tectonic pressure solution (right column, Fig. 10) resulting in an average of 30% bulk volume loss and 3% material volume loss. For all samples, the evidence for an external source for much or all of the cement indicates that the flux of material was considerably greater than the material volume change.

*Acknowledgements*—This research was supported by NSF grants EAR-8500389 and EAR-8915949. The manuscript was improved by the comments of two anonymous reviewers.

## REFERENCES

Ague, J. J. 1991. Evidence of major mass transfer and volume strain during regional metamorphism of pelites. *Geology* **19**, 855–858.

Alvarez, W., Engelder, T. & Geiser, P. A. 1978. Classification of solution cleavage in pelagic limestones. *Geology* **6**, 263–266.

Atkinson, B. K. & Rutter, E. H. 1975. "Pressure solution" or indentation?—Discussion. *Geology* **3**, 477–478.

Beard, D. C. & Weyl, P. K. 1973. Influence of texture on porosity and permeability of unconsolidated sand. *Am. Ass. Petrol. Geol.* **57**, 349–369.

Beutner, E. C. & Charles, E. G. 1985. Large volume loss during cleavage formation, Hamburg sequence, Pennsylvania. *Geology* **13**, 803–805.

Boulter, C. A. 1983. Compaction-sensitive accretionary lapilli: a means for recognizing soft-sedimentary deformation. *J. geol. Soc. Lond.* **140**, 789–794.

Boulter, C. A. 1986. Accretionary lapilli-filled clastic dikes: a comparison of compaction strain estimates from dyke folding and lapilli shape factors. *J. Struct. Geol.* **8**, 201–204.

Brandon, M. T., Feehan, J. & Paterson, S. 1991. Volume strains associated with pressure-solution deformation in sandstones from high P–low T terrains: A third of the rock is missing! *Geol. Soc. Am. Abs. w. Prog.* **23**, 362.

Chandra, S. K., Bhattacharyya, A. & Sarkar, S. 1977. Deformation of ooids by compaction in the Precambrian Bhander Limestone, India: Implications for lithification. *Bull. geol. Soc. Am.* **88**, 1577–1585.

Couzens, B. A., Dunne, W. M., Onasch, C. M. & Glass, R. 1993. Strain variations and three-dimensional strain factorization at the transition from the southern to central Appalachians. *J. Struct. Geol.* **15**, 451–464.

Cox, S. F. & Ethridge, M. A. 1989. Coupled grain-scale dilatancy and mass transfer during deformation at high fluid pressures: examples from Mount Lyell, Tasmania. *J. Struct. Geol.* **11**, 147–162.

Dean, S. L., Kulander, B. R. & Skinner, J. M. 1988. Structural chronology of the Alleghanian orogeny in southeastern West Virginia. *Bull. geol. Soc. Am.* **100**, 299–310.

Deelman, J. C. 1975. "Pressure solution" or indentation. *Geology* **3**, 23–24.

Durney, D. W. 1976. Pressure-solution and crystallization deformation. *Phil. Trans. R. Soc. Lond.* **A283**, 229–240.

Epstein, A. G., Epstein, J. B. & Harris, L. D. 1977. Conodont color alteration—an index to organic metamorphism. *Prof. Pap. U.S. geol. Surv.* **995**.

Epstein, R. L. 1988. Illite crystallinity of the Middle and Upper Ordovician allochthonous and autochthonous rocks in the Great Valley of central Pennsylvania. Unpublished M.Sc. thesis, Bowling Green State University, Ohio.

Gaither, A. 1953. A study of porosity and grain relationships in experimental sands. *J. sedim. Petrol.* **23**, 180–195.

Geiser, P. A. & Engelder, T. 1983. The distribution of layer-parallel shortening fabrics in the Appalachian foreland of New York and Pennsylvania; evidence for two, non-coaxial phases of Alleghanian orogeny. In: *Contributions to the Tectonics and Geophysics of Mountain Chains* (edited by Hatcher, R. D., Williams, H. & Zeitz, I.). *Mem. geol. Soc. Am.* **158**, 161–175.

Graton, L. C. & Frasier, H. J. 1935. Systematic packing of spheres with particular relation to porosity and permeability. *J. Geol.* **43**, 785–909.

Harris, A. G. 1979. Conodont color alteration, an organo-mineral metamorphic index, and its application to Appalachian Basin geology. In: *Aspects of Diagenesis* (edited by Scholle, P. A. & Schluger, P. R.). *Spec. Publ. Soc. econ. Petrol. Miner.* **26**, 3–16.

Hatcher, R. D., Jr, Thomas, W. A., Geiser, P. A., Snoke, A. W., Moser, S. & Wiltschko, D. V. 1989. Alleghanian orogen: In: *The Appalachian–Ouachita Orogen in the United States* (edited by Hatcher, R. D. Jr, Thomas, W. A. & Viele, G. W.). *Geol. Soc. Am., The Geology of North America* **F-2**, 223–318.

Heald, M. T. 1956. Cementation of Simpson and St. Peter sandstones in parts of Oklahoma, Arkansas, and Missouri. *J. Geol.* **64**, 16–30.

Henderson, J. R., Wright, T. O. & Henderson, M. N. 1986. A history of cleavage and folding: An example from the Goldenville Formation, Nova Scotia. *Bull. geol. Soc. Am.* **97**, 1354–1366.

Houseknecht, D. W. 1988. Intergranular pressure solution in four quartzose sandstones. *J. sedim. Petrol.* **58**, 228–246.

Jamison, W. R. 1989. Fault-fracture strain in Wingate Sandstone. *J. Struct. Geol.* **11**, 959–974.

Kerrich, R. 1977. An historical review and synthesis of research on pressure solution. *Zentbl. Miner. Geol. Paläont.* **5**, 512–550.

Lawn, B. R. & Wilshaw, T. R. 1975. *Fracture of Brittle Solids*. Cambridge University Press, Cambridge.

Lloyd, G. E. & Knipe, R. J. 1992. Deformation mechanism accommodating faulting of quartzite under upper crustal conditions. *J. Struct. Geol.* **14**, 127–143.

Manus, R. W. & Coogan, A. H. 1974. Bulk volume reduction and pressure solution derived cement. *J. Sedim. Petrol.* **44**, 466–471.

Marrett, R. & Allmendinger, R. W. 1990. Kinematic analysis of fault-slip data. *J. Struct. Geol.* **12**, 973–986.

Mitra, S. & Beard, W. C. 1980. Theoretical models of porosity reduction by pressure solution for well-sorted sandstones. *J. Sedim. Petrol.* **50**, 1347–1360.

Mosher, S. 1987. Pressure-solution deformation of the Purgatory Conglomerate, Rhode Island (U.S.A.): quantification of volume change, real strains and sedimentary shape factor. *J. Struct. Geol.* **9**, 221–232.

Oertel, G. 1970. Deformation of a slaty, lapillar tuff in the Lake District, England. *Bull. geol. Soc. Am.* **81**, 1173–1188.

Onasch, C. M. 1990. Microfractures and their role in deformation of a quartz arenite from the central Appalachian foreland. *J. Struct. Geol.* **12**, 883–894.

Onasch, C. M. 1991. Anatomy of a fold: The Massanutten synclinorium in northwest Virginia. *Geol. Soc. Am. Abs. w. Prog.* **23**, 112.

Onasch, C. M. In press. Determination of pressure solution shortening in sandstones. *Tectonophysics*.

Onasch, C. M. & Dunne, W. M. 1993. Variation in quartz arenite deformation mechanisms between a roof sequence and duplexes. *J. Struct. Geol.* **15**, 465–475.

Ramsay, J. G. & Wood, D. S. 1976. The geometric effects of volume change during deformation processes. *Tectonophysics* **16**, 263–277.

Sanderson, D. J. 1976. The superposition of compaction and plane strain. *Tectonophysics* **30**, 35–54.

Sibley, D. F. & Blatt, H. 1976. Intergranular pressure solution and cementation of the Tuscarora orthoquartzite. *J. sedim. Petrol.* **46**, 881–896.

Sibson, R. H. 1987. Earthquake rupturing as a mineralizing agent in hydrothermal systems. *Geology* **15**, 701–704.

Wilson, T. V. & Sibley, D. F. 1978. Pressure solution and porosity reduction in shallow buried quartz arenite. *Bull. Am. Ass. Petrol. Geol.* **62**, 2329–2334.

Wintsch, R. P., Kvale, C. M. & Kisch, H. D. 1991. Open-system, constant volume development of slaty cleavage, and strain-induced replacement reactions in the Martinsburg Formation, Lehigh Gap, Pennsylvania. *Bull. geol. Soc. Am.* **103**, 916–927.

Wojtal, S. 1986. Deformation within foreland thrust sheets by populations of minor faults: *J. Struct. Geol.* **8**, 426–435.

Wojtal, S. 1989. Measuring displacement gradients and strains in faulted rocks. *J. Struct. Geol.* **11**, 669–678.

Wright, T. O. & Henderson, J. R. 1992. Volume loss during cleavage formation in Meguma Group, Nova Scotia, Canada. *J. Struct. Geol.* **14**, 281–290.

Wright, T. O. & Platt, L. B. 1982. Pressure dissolution and cleavage in the Martinsburg Shale. *Am. J. Sci.* **282**, 122–135.